

Mixed quantum-classical methods for treating coherent quantum dynamics in model multi-chromophore light harvesting systems

David F. Coker

Department of Chemistry, Boston University

Department of Physics, University College Dublin

New CECAM node: ACAM (acam.ie)

Thanks to: Sara Bonella, Emily Dunkel, Pengfei (Frank) Huo

Funding: NSF, SFI, UCD

Warwick Workshop on Molecular Dynamics:
Warwick MRC, UK June 1-5, 2009

Outline:

- (0) Mixed quantum-classical dynamics methods that can represent environmental coherence effects
- (1) Motivation: Collective long-range environmental response apparently responsible for long-lived quantum coherent dynamics in photosynthetic antenna arrays
- (2) Iterating “short” time linearized propagators for long time density matrix dynamics, Monte Carlo density matrix element sampling & taming the exponential growth of trajectories.
- (3) Mixed QC non-adiabatic model calculations: Driven nonequilibrium multidimensional environment can prolong condensed phase quantum coherent dynamics.

Quantum Mechanics (4): Entangled states & interaction with environment (relationship to measurement)

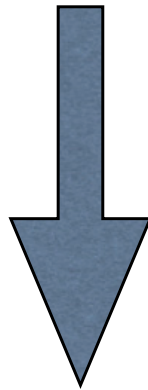
(initially separable)

$$\Psi(0) = (\psi_1(r) + \psi_2(r))\chi(R) = \psi_1(r)\chi(R) + \psi_2(r)\chi(R)$$

subsystem (r) in
superposition state

State of environment

$$i\hbar \frac{\partial}{\partial t} \Psi = \hat{H} \Psi$$



$$\Psi(t) = \psi_1(r, t)\chi_1(R, t) + \psi_2(r, t)\chi_2(R, t)$$

Non-separable ENTANGLED state



“Schroedinger’s Cat”

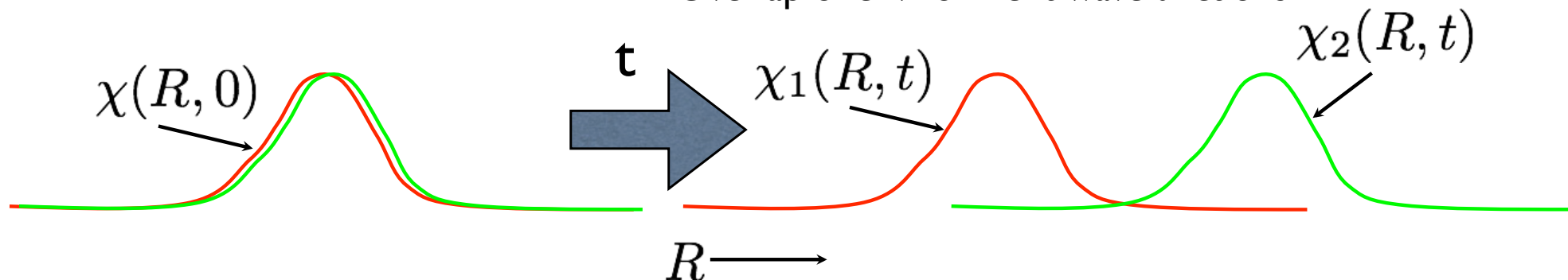
Quantum Mechanics (5):

Quantum DECOHERENCE, environment interactions collapse the wave function!

Only study the system (sum over all realizations of the environment)

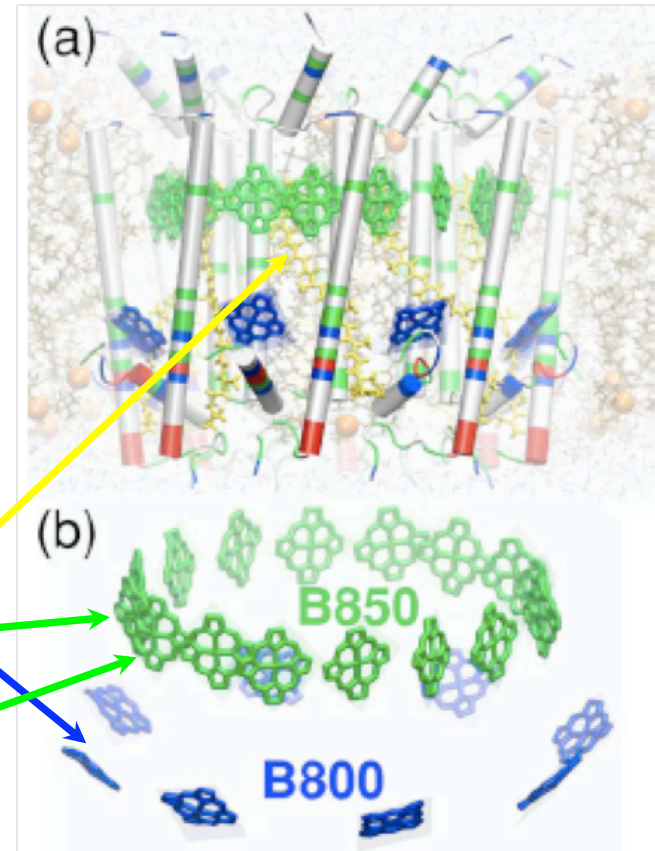
$$\begin{aligned}
 P_{red}(r, t) &= \int dR |\Psi(t)|^2 \\
 &= |\psi_1(r, t)|^2 \int dR |\chi_1(R, t)|^2 \\
 &\quad + |\psi_2(r, t)|^2 \int dR |\chi_2(R, t)|^2 \\
 &\quad + 2\psi_1(r, t)\psi_2(r, t) \int dR \chi_1(R, t)\chi_2(R, t)
 \end{aligned}$$

Overlap of environment wavefunctions



“Spin-Boson” model for exciton transport, dissipation, and decoherence in antenna arrays

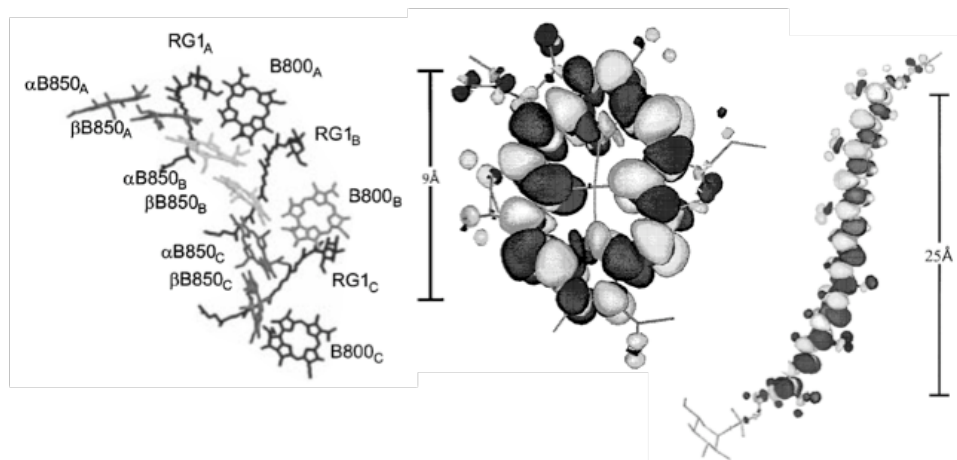
$$\begin{aligned}
 \hat{H} = & \sum_n \hbar \omega_n (\hat{b}_n^\dagger \hat{b}_n + 1/2) \\
 & + [\epsilon_D + \sum_n \hbar g_{n,D} (\hat{b}_n + \hat{b}_n^\dagger)] |D\rangle \langle D| \\
 & + [\epsilon_\alpha + \sum_n \hbar g_{n,\alpha} (\hat{b}_n + \hat{b}_n^\dagger)] |A_\alpha\rangle \langle A_\alpha| \\
 & + [\epsilon_\beta + \sum_n \hbar g_{n,\beta} (\hat{b}_n + \hat{b}_n^\dagger)] |A_\beta\rangle \langle A_\beta| \\
 & + [\Delta_{\alpha\beta} + \sum_n \hbar g_{n,\alpha\beta}^\Delta (\hat{b}_n + \hat{b}_n^\dagger)] (|A_\alpha\rangle \langle A_\beta| + |A_\beta\rangle \langle A_\alpha|) \\
 & + [J_{D\alpha} + \sum_n \hbar g_{n,\alpha}^J (\hat{b}_n + \hat{b}_n^\dagger)] (|D\rangle \langle A_\alpha| + |A_\alpha\rangle \langle D|) \\
 & + [J_{D\beta} + \sum_n \hbar g_{n,\beta}^J (\hat{b}_n + \hat{b}_n^\dagger)] (|D\rangle \langle A_\beta| + |A_\beta\rangle \langle D|)
 \end{aligned}$$



LHC2

c.f. Jang, Newton, Silbey
J. Phys. Chem. B, 111, 6807 (2007)

$$J_{D\alpha} = \frac{\mu_D \cdot \mu_\alpha - 3(\mu_D \cdot \hat{R}_{D\alpha})(\mu_\alpha \cdot \hat{R}_{D\alpha})}{\epsilon R_{D\alpha}^3}$$



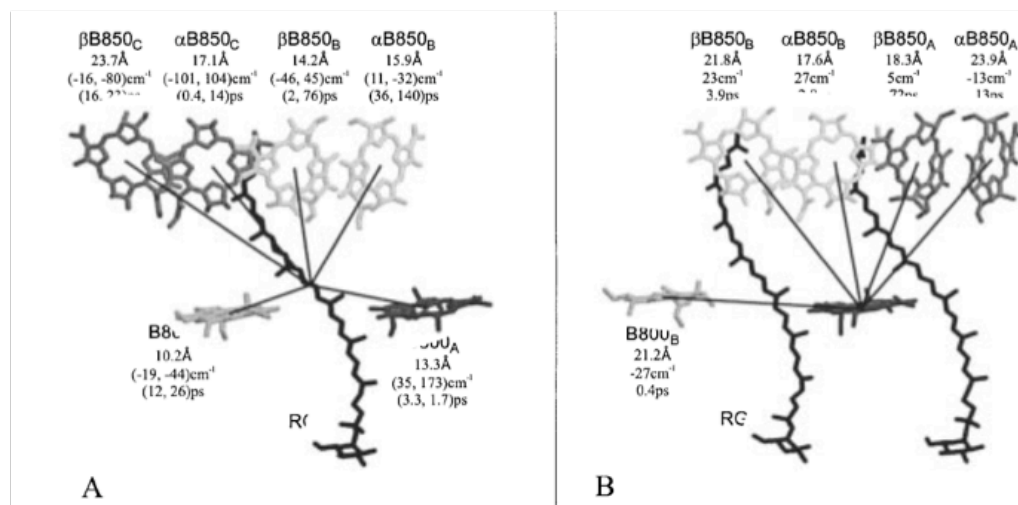
5378

J. Phys. Chem. B 1998, 102, 5378–5386

Calculation of Couplings and Energy-Transfer Pathways between the Pigments of LH2 by the *ab Initio* Transition Density Cube Method

Brent P. Krueger, Gregory D. Scholes, and Graham R. Fleming*

Parameters for
models for use
in approximate
theories
Obtained from
detailed
spectroscopy
and *ab initio*
calculations



Coupling strengths and energy transfer times from the RG1B S2 (A) and B800A Qy (B) transitions to nearby Bchl a transitions. Shading of the chromophores is as in Figure 2. Near each acceptor pigment is given the label, center-to-center separation, coupling strength V_{Coul} , and transfer time. For transfer from RG S2, the interaction with both the Qx and Qy transitions of the acceptor is given (Qx, Qy), whereas for B800 Qy only interaction with the acceptor Qy transition is given.

Coherence Dynamics in Photosynthesis: Protein Protection of Excitonic Coherence

Hohjai Lee, Yuan-Chung Cheng, Graham R. Fleming*

Science, 316, 1462 (2007)

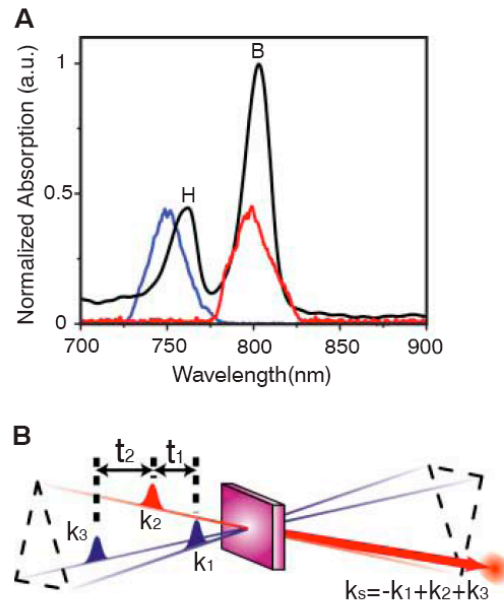


Fig. 1. The 2CECPE experiment. **(A)** The 77 K absorption spectrum (black) of the P-oxidized RC from the photosynthetic purple bacterium *R. sphaeroides* and the spectral profiles of the ~40-fs laser pulses (blue, 750 nm; red, 800 nm) used in the experiment. **(B)** The pulse sequence for the 2CECPE experiment. We detect the integrated intensity in the phase-matched direction $k_s = -k_1 + k_2 + k_3$. a.u., arbitrary units.

states. We applied the method to the coherence between bacteriopheophytin and accessory bacteriochlorophyll in the purple bacteria reaction center (RC). The measurement quantifies dephasing dynamics in the system and provides strong evidence that the collective long-range electrostatic response of the protein environment to the electronic excitations is responsible for the long-lasting quantum coherence. In other words, the protein environment protects electronic coherences and plays a role in the optimization of excitation energy transfer in photosynthetic complexes.

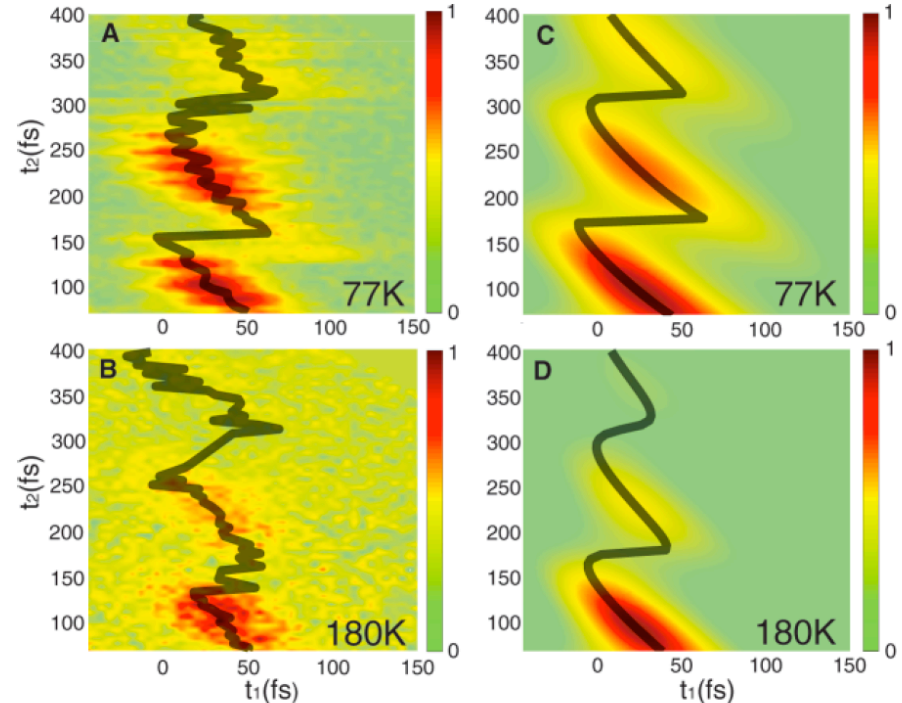


Fig. 2. Two-dimensional maps of experimental **(A and B)** and simulated **(C and D)** integrated echo signals as a function of the two delay times, t_1 and t_2 , from the RC. The black lines follow the maximum of the echo signal at a given t_2 . The data at $t_2 < 75$ fs are not shown because the conventional two-color three-pulse photon echo signal (750-750-800 nm) overwhelms the 2CECPE signal in this region, due to the pulse overlap effect.

PREVIOUS METHODS: 1/3

◎ Forster resonance energy transfer (FRET) theory

Multi-Chromophore FRET

$$k^{\text{MC}}(t) = \sum_{j'j''} \sum_{k'k''} \frac{J_{jk'} J_{j''k''}}{2\pi\hbar^2} \int_{-\infty}^{\infty} d\omega E_D^{j''j'}(t, \omega) I_A^{k'k''}(\omega),$$

$$I_A^{k'k''}(\omega) \equiv \int_{-\infty}^{\infty} dt e^{i\omega t} \text{Tr}_A \{ e^{iH_A^g t/\hbar} \langle A_{k'} | e^{-iH_A^e t/\hbar} | A_{k''} \rangle \rho_A^g \},$$

$$E_D^{j''j'}(t, \omega) = 2\text{Re} \left[\int_0^t dt' e^{-i\omega t'} \text{Tr}_D \{ e^{-iH_D^g t'/\hbar} \langle D_{j'} | \right. \\ \left. \times e^{-iH_D^e(t-t')/\hbar} | D_{j''} \rangle \langle D_{j''} | \rho_D^g e^{iH_D^e t'/\hbar} | D_{j'} \rangle \} \right],$$

◎ Comments:

- Time dependent perturbation theory
 - May not valid for strong coupling situation
- Ignores quantum coherent dynamics !!

SJ Jang, MD Newton, and RJ Silbey. Multichromophoric Forster resonance energy transfer. *PHYSICAL REVIEW LETTERS*, 92(21), MAY 28 2004.

PREVIOUS METHODS: 2/3

◉ Extension of Redfield theory

Nakajima-Zwanzig equation

$$\mathcal{P}W(t) = R_{\text{eq}} \text{tr}_B\{W(t)\} = R_{\text{eq}}\rho(t) \quad Q = 1 - \mathcal{P} \quad \frac{\partial}{\partial t}\mathcal{P}W(t) = -i\mathcal{P}\mathcal{L}\mathcal{P}W(t) - \int_0^t d\tau \mathcal{P}\mathcal{L}e^{-iQ\mathcal{L}(t-\tau)}Q\mathcal{L}\mathcal{P}W(\tau)$$

◉ Redfield Equation :

$$\begin{aligned} \frac{d\sigma_{ab}}{dt} = & -i\omega_{ab}\sigma_{ab} - \frac{i}{\hbar} \sum_c (\hat{V}_{ac}\sigma_{cb} - \sigma_{ac}\hat{V}_{cb}) \\ & - \sum_{c,d} (R_{ac,cd}(\omega_{dc})\sigma_{db}(t) + R_{bd,dc}^*(\omega_{cd})\sigma_{ac}(t)) \\ & - [R_{db,ac}(\omega_{ca}) + R_{ca,bd}^*(\omega_{db})]\sigma_{cd}(t) \end{aligned}$$

$$R_{ab,cd}(\omega) + R_{dc,ba}^*(\omega) = \int_{-\infty}^{\infty} dt e^{i\omega t} M_{ab,cd}(t)$$

$$M_{ab,cd}(t) \equiv \frac{1}{\hbar^2} C(t) V_{ab}^s V_{cd}^s \quad C(t) = \langle V(0) \cdot V(t) \rangle \quad V = \hat{H}_B + \hat{H}_{s-B}$$

- ◉ Includes Markovian approximation
- ◉ Valid only for bath mode moving faster than exciton transfer time scale
- ◉ Does not necessarily conserve the positivity property

PREVIOUS METHODS: 3/3

- Methods based on the **Lindblad master equation**

$$\dot{\hat{\sigma}} = -\frac{i}{\hbar} [\hat{H}_0, \hat{\sigma}] + \frac{1}{2} \sum_j \left(\left[\hat{V}_j \hat{\sigma}, \hat{V}_j^\dagger \right] + \left[\hat{V}_j, \hat{\sigma} \hat{V}_j^\dagger \right] \right)$$

- A linear Markovian time evolution
- Conserve the positivity

PHYSICAL REVIEW B **78**, 085115 2008

Various alternative approximations to evolve the reduced density matrix based on the **Liouville-von Neumann equation**

Iterative linearized density matrix dynamics

J. Chem. Phys. 114 106 (2008)

$$\hat{\rho}(2t) = e^{-\frac{i}{\hbar} \hat{H}t} e^{-\frac{i}{\hbar} \hat{H}t} \hat{\rho}(0) e^{\frac{i}{\hbar} \hat{H}t} e^{\frac{i}{\hbar} \hat{H}t}$$

$$\hat{H} = \hat{P}^2/2M + \hat{h}(\hat{R}) = \hat{P}^2/2M + \sum_n \sum_m |n\rangle h_{nm}(\hat{R}) \langle m|$$

$$\langle R_{2t} n_{2t} | \hat{\rho}(2t) | R'_{2t} n'_{2t} \rangle =$$

$$\begin{aligned} & \sum_{n_t, n'_t} \int dR_t dR'_t \sum_{n_0, n'_0} \int dR_0 dR'_0 \langle R_{2t} n_{2t} | e^{-\frac{i}{\hbar} \hat{H}t} | R_t n_t \rangle \langle R_t n_t | e^{-\frac{i}{\hbar} \hat{H}t} | R_0 n_0 \rangle \\ & \times \langle R_0 n_0 | \hat{\rho}(0) | R'_0 n'_0 \rangle \langle R'_0 n'_0 | e^{\frac{i}{\hbar} \hat{H}t} | R'_t n'_t \rangle \langle R'_t n'_t | e^{\frac{i}{\hbar} \hat{H}t} | R'_{2t} n'_{2t} \rangle \end{aligned}$$

Mapping Hamiltonian formulation

$$|n\rangle \rightarrow |m_n\rangle = |0_1, \dots, 1_n, \dots, 0_{N_s}\rangle \quad \hat{H}_m = \hat{P}^2/2M + \hat{h}_m(\hat{R})$$

$$\begin{aligned} \hat{h}_m(\hat{R}) = & \frac{1}{2} \sum_{\lambda} h_{\lambda, \lambda}(\hat{R}) (\hat{q}_{\lambda}^2 + \hat{p}_{\lambda}^2 - \hbar) \\ & + \frac{1}{2} \sum_{\lambda, \lambda'} h_{\lambda, \lambda'}(\hat{R}) (\hat{q}_{\lambda'} \hat{q}_{\lambda} + \hat{p}_{\lambda'} \hat{p}_{\lambda}) \end{aligned}$$

Time slice forward and
backward propagators

$$\epsilon = t/N$$

$$\langle R_k | e^{-\frac{i}{\hbar} \hat{H}_m \epsilon} | R_{k-1} \rangle = \int \frac{dP_k}{2\pi\hbar} e^{\frac{i}{\hbar} [P_k (R_k - R_{k-1}) - \epsilon \frac{P_k^2}{2M}]} e^{-\frac{i\epsilon}{\hbar} \hat{h}_m(R_{k-1})}$$

$$\begin{aligned} \langle R_N m_{n_t} | e^{-\frac{i}{\hbar} \hat{H}_m t} | R_0 m_{n_0} \rangle = \\ \int \prod_{k=1}^{N-1} dR_k \frac{dP_k}{2\pi\hbar} \frac{dP_N}{2\pi\hbar} e^{\frac{i}{\hbar} S_0} \langle m_{n_t} | e^{-\frac{i}{\hbar} \epsilon \hat{h}_m(R_{N-1})} \dots e^{-\frac{i}{\hbar} \epsilon \hat{h}_m(R_0)} | m_{n_0} \rangle \end{aligned}$$

$$S_0 = \epsilon \sum_{k=1}^N \left[P_k \frac{(R_k - R_{k-1})}{\epsilon} - \frac{P_k^2}{2M} \right]$$

Transition amplitudes

$$\langle m_{n_t} | e^{-\frac{i}{\hbar} \epsilon \hat{h}_m(R_{N-1})} \dots e^{-\frac{i}{\hbar} \epsilon \hat{h}_m(R_0)} | m_{n_0} \rangle =$$

$$\int dq_0 dp_0 r_{t,n_t}(\{R_k\}) e^{-i\Theta_{t,n_t}(\{R_k\})} r_{0,n_0} e^{i\Theta_{0,n_0}} G_0$$

Magnitude

$$G_0 = e^{-\frac{1}{2} \sum_{\lambda} (q_{0,\lambda}^2 + p_{0,\lambda}^2)}$$

$$r_{t,n_t}(\{R_k\}) = \sqrt{q_{t,n_t}^2(\{R_k\}) + p_{t,n_t}^2(\{R_k\})}$$

Phase

$$\Theta_{t,n_t}(\{R_k\}) =$$

$$\tan^{-1} \left(\frac{p_{0,n_t}}{q_{0,n_t}} \right) + \int_0^t d\tau h_{n_t,n_t}(R_{\tau}) + \int_0^t d\tau \sum_{\lambda \neq n_t} \left[h_{n_t,\lambda}(R_{\tau}) \frac{(p_{\tau n_t} p_{\tau \lambda} + q_{\tau n_t} q_{\tau \lambda})}{(p_{\tau n_t}^2 + q_{\tau n_t}^2)} \right]$$

$$= \tan^{-1} \left(\frac{p_{0,n_t}}{q_{0,n_t}} \right) + \int_0^t \theta_{n_t}(R_{\tau}) d\tau$$

Density matrix propagation: First step

$$\begin{aligned}
 \langle R_N n_t | \hat{\rho}(t) | R'_N n'_t \rangle = & \\
 & \sum_{n_0, n'_0} \int dq_0 dp_0 dq'_0 dp'_0 \int dR_0 dR'_0 \int \prod_{k=1}^{N-1} dR_k \frac{dP_k}{2\pi\hbar} \frac{dP_N}{2\pi\hbar} \int \prod_{k=1}^{N-1} dR'_k \frac{dP'_k}{2\pi\hbar} \frac{dP'_N}{2\pi\hbar} \\
 & \times e^{\frac{i}{\hbar}(S_0 - S'_0)} r'_{0, n'_0} e^{-i\Theta'_{0, n'_0}} G'_0 r_{0, n_0} e^{i\Theta_{0, n_0}} G_0 \langle R_0 n_0 | \hat{\rho}(0) | R'_0 n'_0 \rangle \\
 & \times r_{t, n_t}(\{R_k\}) e^{-i\Theta_{t, n_t}(\{R_k\})} r'_{t, n'_t}(\{R'_k\}) e^{i\Theta'_{t, n'_t}(\{R'_k\})}
 \end{aligned}$$

Mean and difference environmental path variables

$$\begin{aligned}
 \bar{R}_k &= (R_k + R'_k)/2 & Z_k &= R_k - R'_k \\
 \bar{P}_k &= (P_k + P'_k)/2 & Y_k &= P_k - P'_k
 \end{aligned}$$

Action difference linear in Z & Y

$$(S_0 - S'_0) = \bar{P}_N Z_N - \bar{P}_1 Z_0 - \sum_{k=1}^{N-1} (\bar{P}_{k+1} - \bar{P}_k) Z_k - \sum_{k=1}^N \left[\frac{\epsilon}{m} \bar{P}_k - (\bar{R}_k - \bar{R}_{k-1}) \right] Y_k$$

truncate phase difference to linear order in path difference

$$\Theta_{t, n_t}(\{\bar{R}_k + Z_k/2\}) - \Theta'_{t, n'_t}(\{\bar{R}_k - Z_k/2\})$$

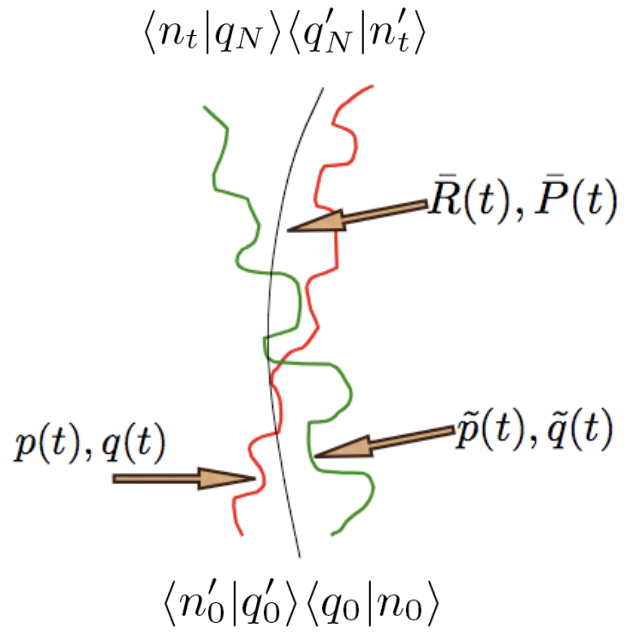
Sample initial conditions from Wigner density

$$(\hat{\rho})_W^{n_0, n'_0}(\bar{R}_0, \bar{P}_1) = \int dZ_0 \langle \bar{R}_0 + \frac{Z_0}{2} n_0 | \hat{\rho} | \bar{R}_0 - \frac{Z_0}{2} n'_0 \rangle e^{-\frac{i}{\hbar} \bar{P}_1 Z_0}$$

First linearized density matrix propagation segment

$$\begin{aligned} \langle \bar{R}_N + \frac{Z_N}{2} n_t | \hat{\rho}(t) | \bar{R}_N - \frac{Z_N}{2} n'_t \rangle = \\ \sum_{n_0, n'_0} \int d\bar{R}_0 dq_0 dp_0 dq'_0 dp'_0 r'_{0, n'_0} e^{-i\Theta'_{0, n'_0}} G'_0 r_{0, n_0} e^{i\Theta_{0, n_0}} G_0 \\ \times \int \prod_{k=1}^{N-1} d\bar{R}_k \frac{d\bar{P}_k}{2\pi} \frac{d\bar{P}_N}{2\pi} [\hat{\rho}]_W^{n_0, n'_0}(\bar{R}_0, \bar{P}_1) e^{i\bar{P}_N Z_N} \\ \times r_{t, n_t}(\{\bar{R}_k\}) r'_{t, n'_t}(\{\bar{R}_k\}) e^{-i\epsilon \sum_{k=1}^N (\theta_{n_t}(\bar{R}_k) - \theta_{n'_t}(\bar{R}_k))} \\ \prod_{i=1}^{J-1} \delta \left(\frac{\bar{P}_{k+1} - \bar{P}_k}{\epsilon} - F_k^{n_t, n'_t} \right) \prod_{k=1}^N \delta \left(\frac{\bar{P}_k}{M} - \frac{\bar{R}_k - \bar{R}_{k-1}}{\epsilon} \right) \end{aligned}$$

Different trajectory forces for different final density matrix elements

$$\begin{aligned}
F_k^{n_t, n'_t} = & -\frac{1}{2} \left\{ \nabla_{\bar{R}_k} h_{n_t, n_t}(\bar{R}_k) + \nabla_{\bar{R}_k} h_{n'_t, n'_t}(\bar{R}_k) \right\} \\
& -\frac{1}{2} \sum_{\lambda \neq n_t} \nabla_{\bar{R}_k} h_{n_t, \lambda}(\bar{R}_k) \left\{ \frac{(p_{n_t k} p_{\lambda k} + q_{n_t k} q_{\lambda k})}{(p_{n_t k}^2 + q_{n_t k}^2)} \right\} \\
& -\frac{1}{2} \sum_{\lambda \neq n'_t} \nabla_{\bar{R}_k} h_{n'_t, \lambda}(\bar{R}_k) \left\{ \frac{(p'_{n'_t k} p'_{\lambda k} + q'_{n'_t k} q'_{\lambda k})}{(p'^2_{n'_t k} + q'^2_{n'_t k})} \right\}
\end{aligned}$$


$\langle n_t | q_N \rangle \langle q'_N | n'_t \rangle$
 $\bar{R}(t), \bar{P}(t)$
 $p(t), q(t)$
 $\tilde{p}(t), \tilde{q}(t)$
 $\langle n'_0 | q'_0 \rangle \langle q_0 | n_0 \rangle$

$$\begin{aligned}
\langle \bar{R}_{2N} + \frac{Z_{2N}}{2} n_{2t} | \hat{\rho}(2t) | \bar{R}_{2N} - \frac{Z_{2N}}{2} n'_{2t} \rangle = & \\
& \sum_{n_t, n'_t} \int d\bar{R}_N dZ_N dq_N dp_N dq'_N dp'_N r'_{t, n'_t} e^{-i\Theta'_{t, n'_t}} G'_t r_{t, n_t} e^{i\Theta_{t, n_t}} G_t \\
& \times \int \prod_{k=N+1}^{2N-1} d\bar{R}_k \frac{d\bar{P}_k}{2\pi} \frac{d\bar{P}_{2N}}{2\pi} \langle \bar{R}_N + \frac{Z_N}{2} n_t | \hat{\rho}(t) | \bar{R}_N - \frac{Z_N}{2} n'_t \rangle e^{i\bar{P}_{N+1} Z_N} \\
& \times e^{-i\bar{P}_{2N+1} Z_{2N}} r_{2t, n_{2t}}(\{\bar{R}_k\}) r'_{2t, n'_{2t}}(\{\bar{R}_k\}) e^{-i\epsilon \sum_{k=N+1}^{2N} (\theta_{n_{2t}}(\bar{R}_k) - \theta_{n'_{2t}}(\bar{R}_k))} \\
& \times \prod_{k=N+1}^{2N-1} \delta \left(\frac{\bar{P}_{k+1} - \bar{P}_k}{\epsilon} - F_k^{n_{2t}, n'_{2t}} \right) \prod_{k=N+1}^{2N} \delta \left(\frac{\bar{P}_k}{M} - \frac{\bar{R}_k - \bar{R}_{k-1}}{\epsilon} \right)
\end{aligned}$$

Second linearized density matrix propagation segment

$$\begin{aligned}
\langle \bar{R}_{2N} + \frac{Z_{2N}}{2} n_{2t} | \hat{\rho}(2t) | \bar{R}_{2N} - \frac{Z_{2N}}{2} n'_{2t} \rangle &= \int \prod_{k=N+1}^{2N-1} d\bar{R}_k \frac{d\bar{P}_k}{2\pi} \frac{d\bar{P}_{2N}}{2\pi} e^{i\bar{P}_{2N} Z_{2N}} \\
&\quad \times r_{2t, n_{2t}}(\{\bar{R}_k\}) r'_{2t, n'_{2t}}(\{\bar{R}_k\}) e^{-i\epsilon \sum_{k=N+1}^{2N} (\theta_{n_{2t}}(\bar{R}_k) - \theta_{n'_{2t}}(\bar{R}_k))} \\
&\quad \times \prod_{k=N+1}^{2N-1} \delta\left(\frac{\bar{P}_{k+1} - \bar{P}_k}{\epsilon} - F_k^{n_{2t}, n'_{2t}}\right) \prod_{k=N+1}^{2N} \delta\left(\frac{\bar{P}_k}{M} - \frac{\bar{R}_k - \bar{R}_{k-1}}{\epsilon}\right) \\
&\quad \sum_{n_t, n'_t} \int d\bar{R}_N \frac{d\bar{P}_N}{2\pi} dq_N dp_N dq'_N dp'_N r'_{t, n'_t} e^{-i\Theta'_{t, n'_t}} G'_t r_{t, n_t} e^{i\Theta_{t, n_t}} G_t \\
&\quad \times \delta(\bar{P}_N - \bar{P}_{N+1}) \delta\left(\frac{\bar{P}_N}{M} - \frac{\bar{R}_N - \bar{R}_{N-1}}{\epsilon}\right) \\
&\quad \times \int \prod_{k=1}^{N-1} d\bar{R}_k \frac{d\bar{P}_k}{2\pi} r_{t, n_t}(\{\bar{R}_k\}) r'_{t, n'_t}(\{\bar{R}_k\}) e^{-i\epsilon \sum_{k=1}^N (\theta_{n_t}(\bar{R}_k) - \theta_{n'_t}(\bar{R}_k))} \\
&\quad \times \prod_{k=1}^{N-1} \delta\left(\frac{\bar{P}_{k+1} - \bar{P}_k}{\epsilon} - F_k^{n_t, n'_t}\right) \prod_{k=1}^N \delta\left(\frac{\bar{P}_k}{M} - \frac{\bar{R}_k - \bar{R}_{k-1}}{\epsilon}\right) \\
&\quad \times \sum_{n_0, n'_0} \int d\bar{R}_0 dq_0 dp_0 dq'_0 dp'_0 r'_{0, n'_0} e^{-i\Theta'_{0, n'_0}} G'_0 r_{0, n_0} e^{i\Theta_{0, n_0}} G_0 [\hat{\rho}]_W^{n_0, n'_0}(\bar{R}_0, \bar{P}_1)
\end{aligned}$$

An Algorithm:

$$(\sum_{n_t, n'_t} \int dq_N dp_N dq'_N dp'_N)_{n_{2t}, n'_{2t}}$$

Intermediate mapping integrals performed by steepest descent

$$(p_{n_0}^o, q_{n_0}^o) = (1/\sqrt{2}, 1/\sqrt{2}) \quad (p_{n_0}^u, q_{n_0}^u) = (0, 0)$$

Intermediate state sums performed by importance sampled MC

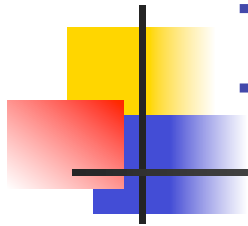
$$r_{\tau, n_t} r'_{\tau, n'_t} \exp[-i \int_0^\tau d\tau' (\theta_{n_t}(\tau') - \theta_{n'_t}(\tau'))]$$

$$M_{n_t, n'_t} = r_{t, n_t} r'_{t, n'_t} / \mathcal{N}(t)$$

$$\mathcal{N}(t) = \sum_{n_t, n'_t} r_{t, n_t} r'_{t, n'_t}$$

Trajectory weights

$$\Omega_K = \left\{ \prod_{k=1}^{K-1} \mathcal{N}(kt) \exp[-i \int_{(k-1)t}^{kt} d\tau' (\theta_{n_{kt}}(\tau') - \theta_{n_{kt}'}(\tau'))] \right\} \\ \times r_{Kt, n_{Kt}} r'_{Kt, n'_{Kt}} \exp[-i \int_{(K-1)t}^{Kt} d\tau' (\theta_{n_{Kt}}(\tau') - \theta_{n'_{Kt}}(\tau'))]$$

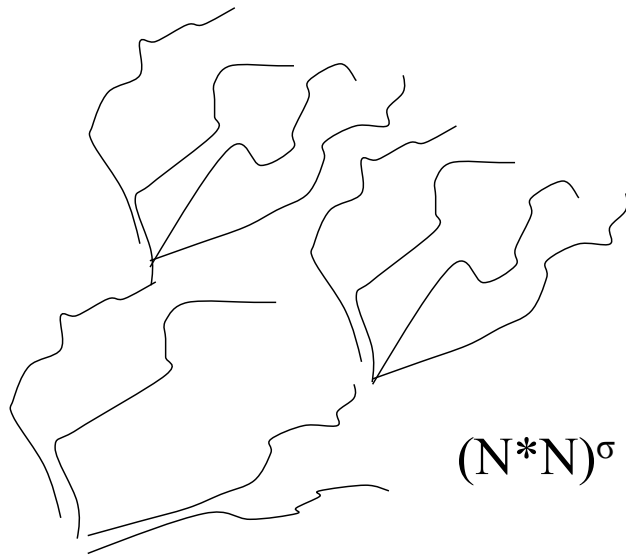


Iterative Scheme LAND-Map

Dunkel et.al 2008

$$\begin{aligned}\langle \hat{O} \rangle_{2t} &= \text{Tr} \{ \hat{\rho}(2t) \hat{O} \} \\ &= \int dR_{2t} \int dR'_{2t} \sum_{n_{2t}} \sum_{n'_{2t}} \langle R_{2t} n_{2t} | \hat{\rho}(2t) | R'_{2t} n'_{2t} \rangle \langle R'_{2t} n'_{2t} | \hat{O} | R_{2t} n_{2t} \rangle\end{aligned}$$

$$\hat{\rho}(2t) = e^{-\frac{i}{\hbar} \hat{H} t} e^{-\frac{i}{\hbar} \hat{H} t} \hat{\rho}(0) e^{\frac{i}{\hbar} \hat{H} t} e^{\frac{i}{\hbar} \hat{H} t}$$

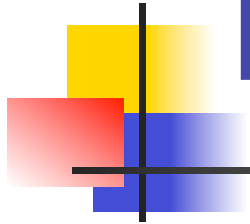


$(N^*N)^\sigma$

$$\begin{aligned}\langle \hat{O} \rangle_{2t} &= \sum_{n_{2t}, n'_{2t}} \int \prod_{k=N+1}^{2N} d\bar{R}_k \frac{d\bar{P}_k}{2\pi\hbar} O_{n_{2t}, n'_{2t}}^W(\bar{R}_{2N}, \bar{P}_{2N}) \\ &\times r_{2t, n_{2t}}(\{\bar{R}_k\}) r'_{2t, n'_{2t}}(\{\bar{R}_k\}) e^{-i\epsilon \sum_{k=N+1}^{2N} (\theta_{n_{2t}}(\bar{R}_k) - \theta_{n'_{2t}}(\bar{R}_k))} \\ &\times \prod_{k=N+1}^{2N-1} \delta\left(\frac{\bar{P}_{k+1} - \bar{P}_k}{\epsilon} - F_k^{n_{2t}, n'_{2t}}\right) \prod_{k=N+1}^{2N} \delta\left(\frac{\bar{P}_k}{M} - \frac{\bar{R}_k - \bar{R}_{k-1}}{\epsilon}\right) \\ &\sum_{n_t, n'_t} \int d\bar{R}_N \frac{d\bar{P}_N}{2\pi\hbar} dq_N dp_N dq'_N dp'_N r'_{t, n'_t} e^{i\Theta'_{t, n'_t} G'_t r_{t, n_t}} e^{-i\Theta_{t, n_t} G_t} \\ &\times \delta(\bar{P}_N - \bar{P}_{N+1}) \delta\left(\frac{\bar{P}_N}{M} - \frac{\bar{R}_N - \bar{R}_{N-1}}{\epsilon}\right) \\ &\times \int \prod_{k=1}^{N-1} d\bar{R}_k \frac{d\bar{P}_k}{2\pi\hbar} r_{t, n_t}(\{\bar{R}_k\}) r'_{t, n'_t}(\{\bar{R}_k\}) e^{-i\epsilon \sum_{k=1}^N (\theta_{n_t}(\bar{R}_k) - \theta_{n'_t}(\bar{R}_k))} \\ &\times \prod_{k=1}^{N-1} \delta\left(\frac{\bar{P}_{k+1} - \bar{P}_k}{\epsilon} - F_k^{n_t, n'_t}\right) \prod_{k=1}^N \delta\left(\frac{\bar{P}_k}{M} - \frac{\bar{R}_k - \bar{R}_{k-1}}{\epsilon}\right) \\ &\times \sum_{n_0, n'_0} \int d\bar{R}_0 dq_0 dp_0 dq'_0 dp'_0 r'_{0, n'_0} e^{i\Theta'_{0, n'_0} G'_0 r_{0, n_0}} e^{-i\Theta_{0, n_0} G_0(\hat{\rho})} G_W^{n_0, n'_0}(\bar{R}_0, \bar{P}_1)\end{aligned}$$

Algorithm: Iterative Scheme

LAND-Map



$$M_{n_t, n'_t} = r_{t, n_t} r'_{t, n'_t} / \sum_{n_t, n'_t} r_{t, n_t} r'_{t, n'_t}$$

$$C_{m_t, m'_t} = \sum_{n_t=1}^{m_t} \sum_{n'_t=1}^{m'_t} M_{n_t, n'_t}$$

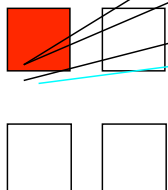
$$\xi \in (0, 1]$$

$$C_{m_t, m'_t} > \xi$$

$$m_t = n_t^* \text{ and } m'_t = n_{t'}^*$$

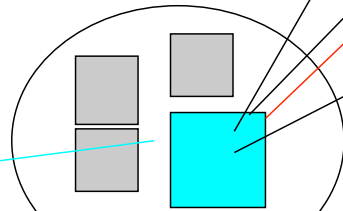
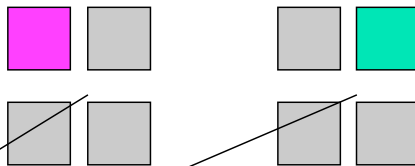
$$\mathcal{N}(2t) \mathcal{N}(t) \exp[-i \int_t^{2t} d\tau (\theta_{n_{2t}^*}(\tau) - \theta_{n_{2t}^*}'(\tau))] \exp[-i \int_0^t d\tau (\theta_{n_t^*}(\tau) - \theta_{n_t^*}'(\tau))]$$

$$\mathcal{N}(t) \exp[-i \int_0^t d\tau (\theta_{n_t}(\tau) - \theta_{n_t}'(\tau))]$$



$$F^{n_t^*, n_{t'}^*}$$

$$(R_0, P_1, n_0, n_0)$$

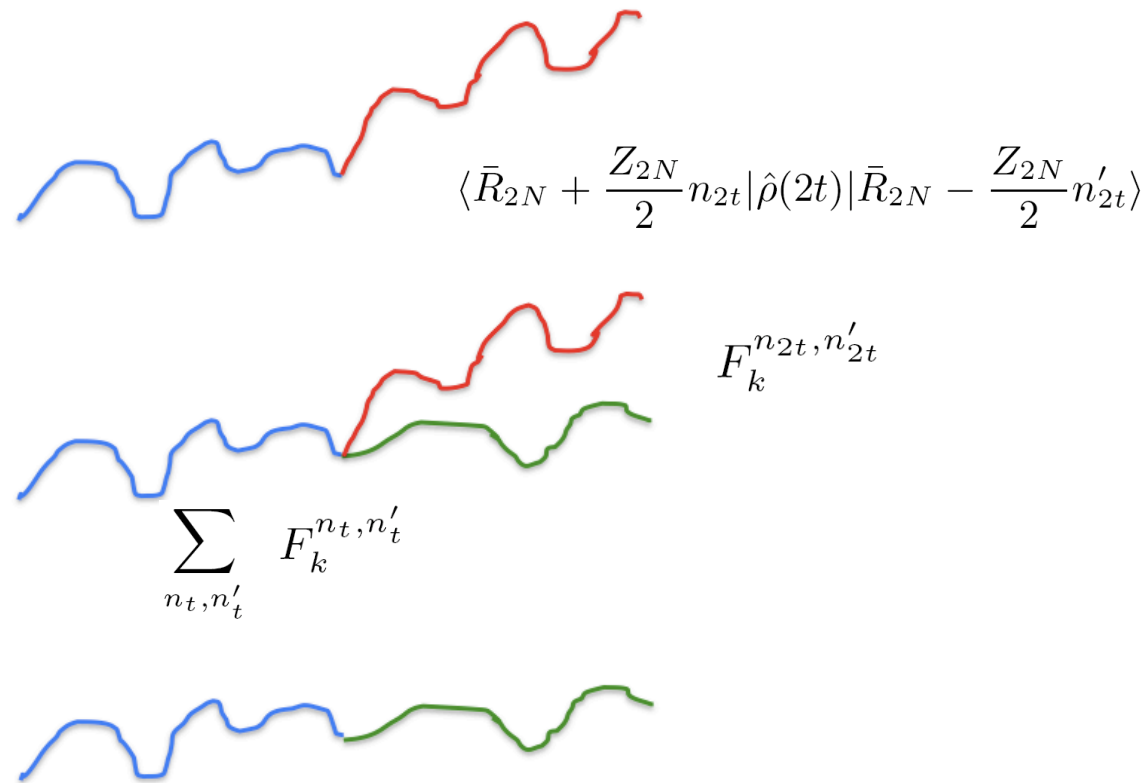


$$(R_N, P_N, n_t^*, n_{t'}^*)$$

$$F^{n_{2t}^*, n_{2t'}^*}$$

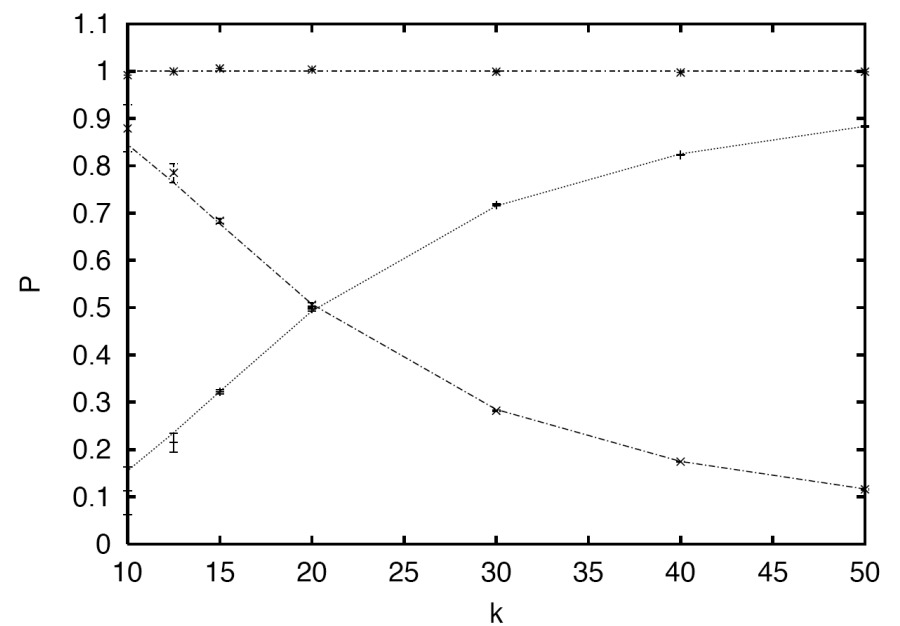
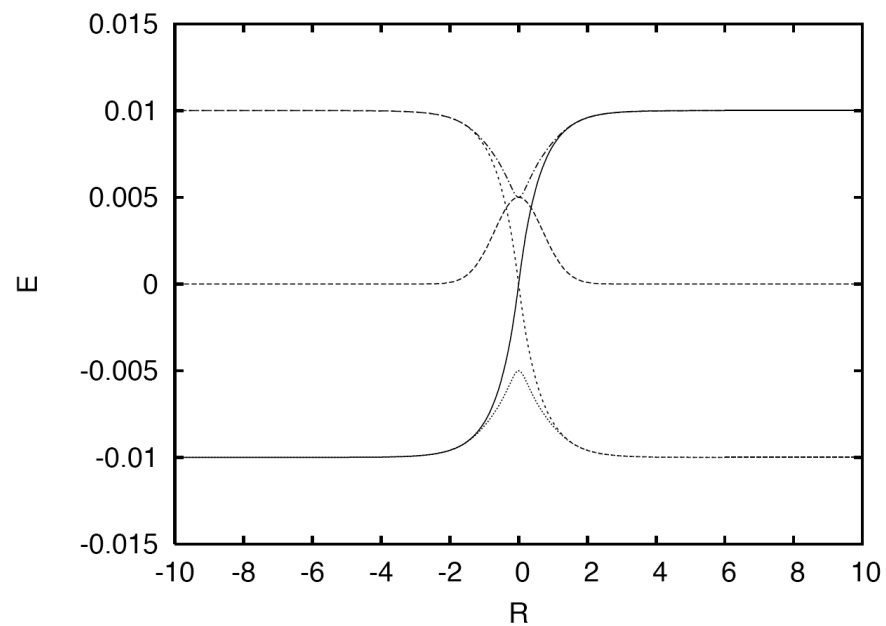
$$(R_{2N}^{(n_{2t}, n_{2t}')}, P_N^{(n_{2t}, n_{2t}')}, n_{2t}, n_{2t}')$$

Sampling different density matrix elements allows forward and backward paths to deviate at longer times when phases of different trajectory segment combinations are added coherently



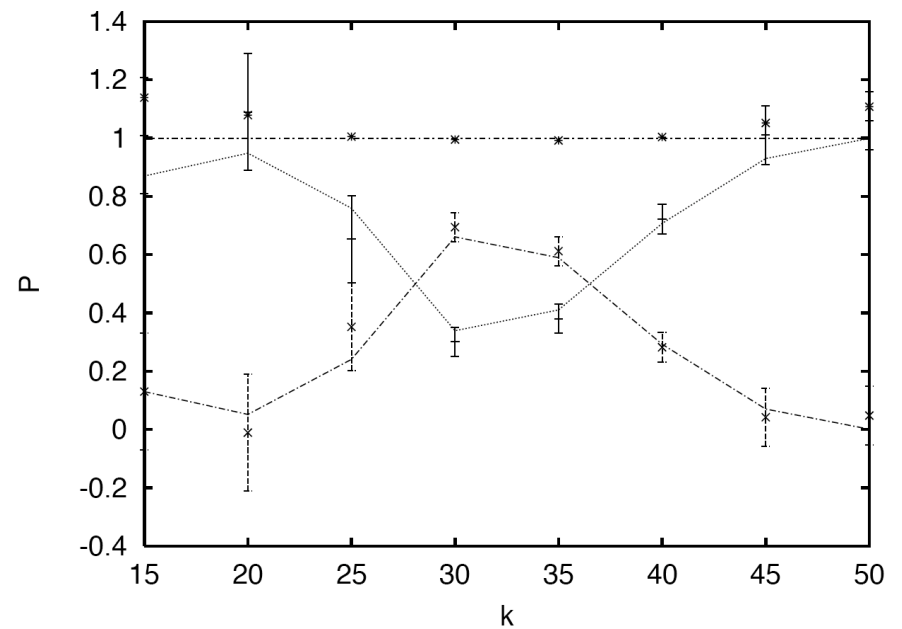
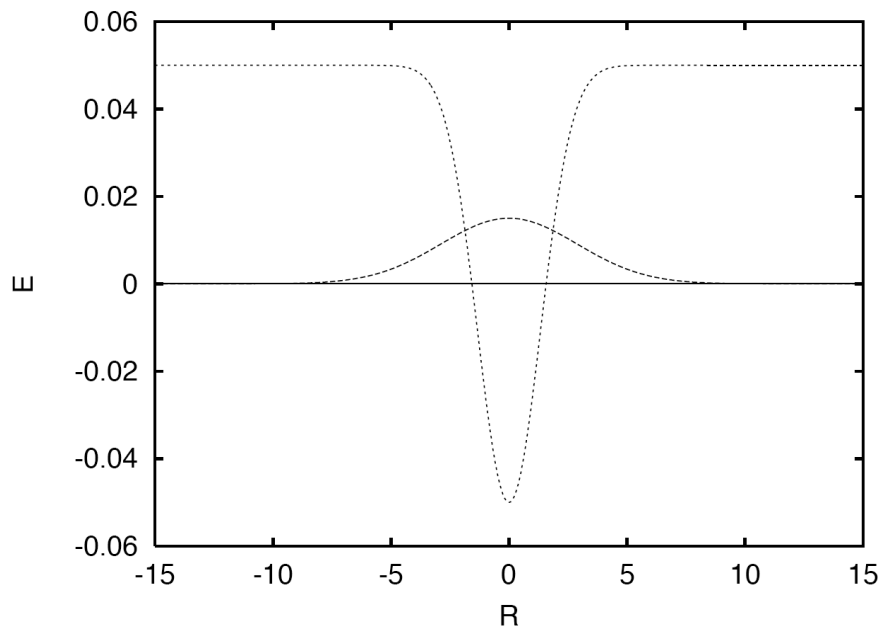
1D Nonadiabatic scattering models

Tully I: 5-15 hop attempt, $N_{\text{traj}} = 5 \times 10^5$

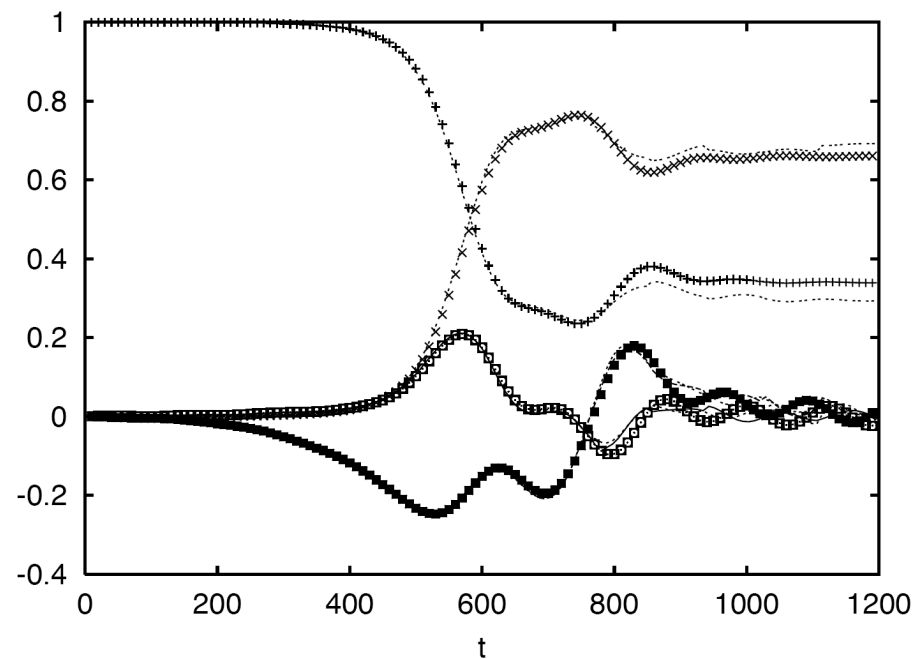


Stuckelberg Scattering model

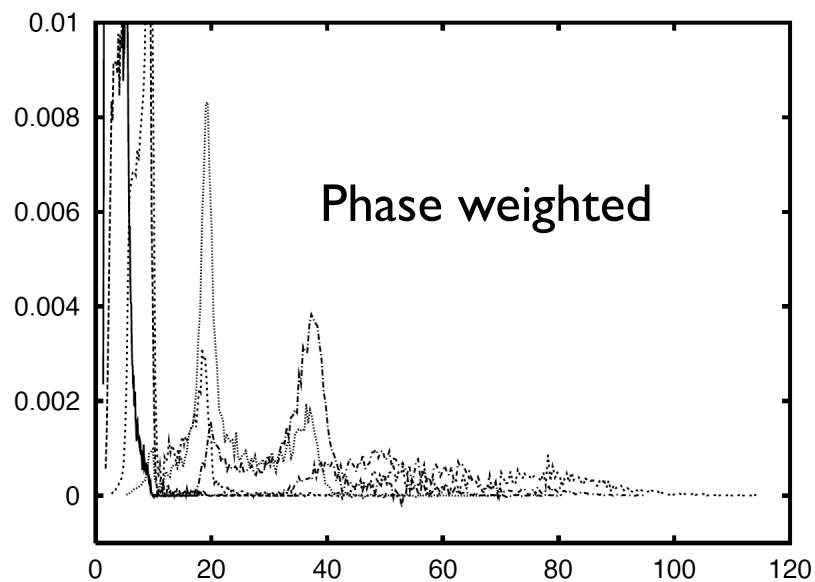
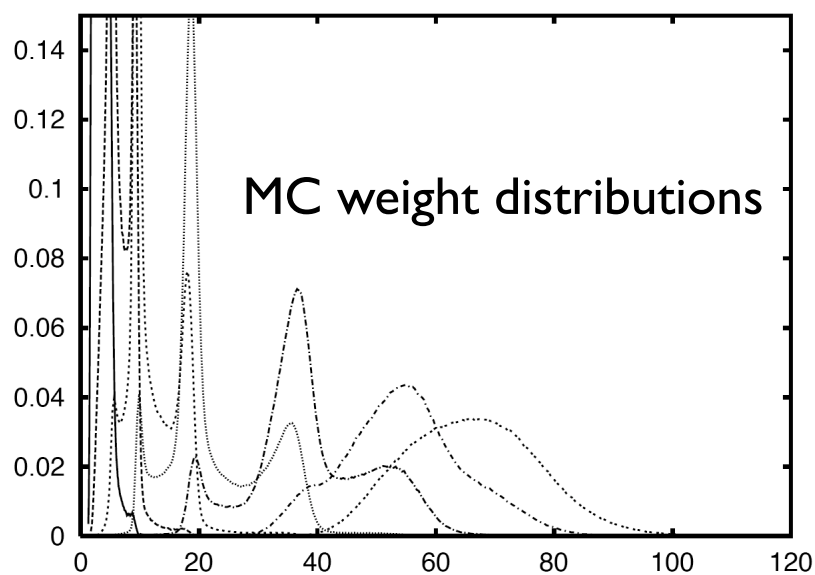
Tully II: 10-20 hop attempt, $N_{\text{traj}} = 1 \times 10^6$



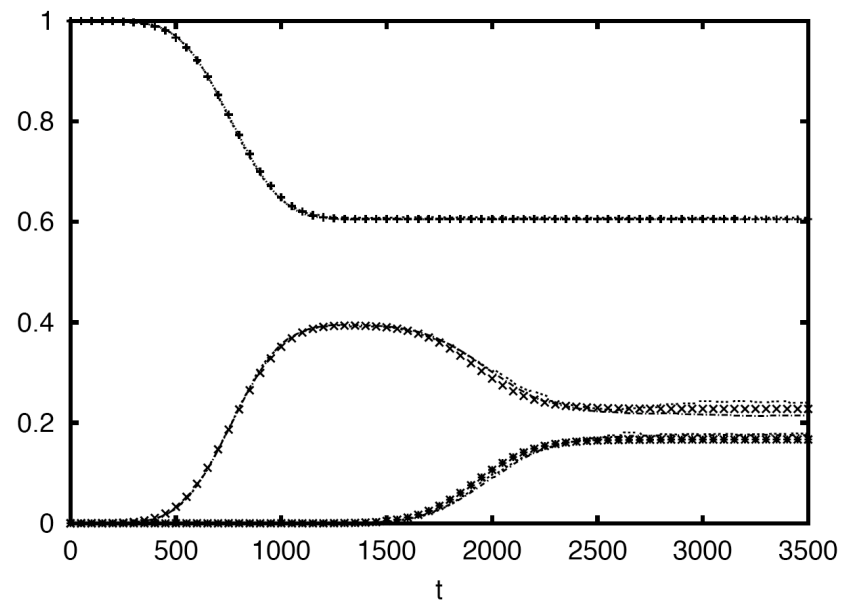
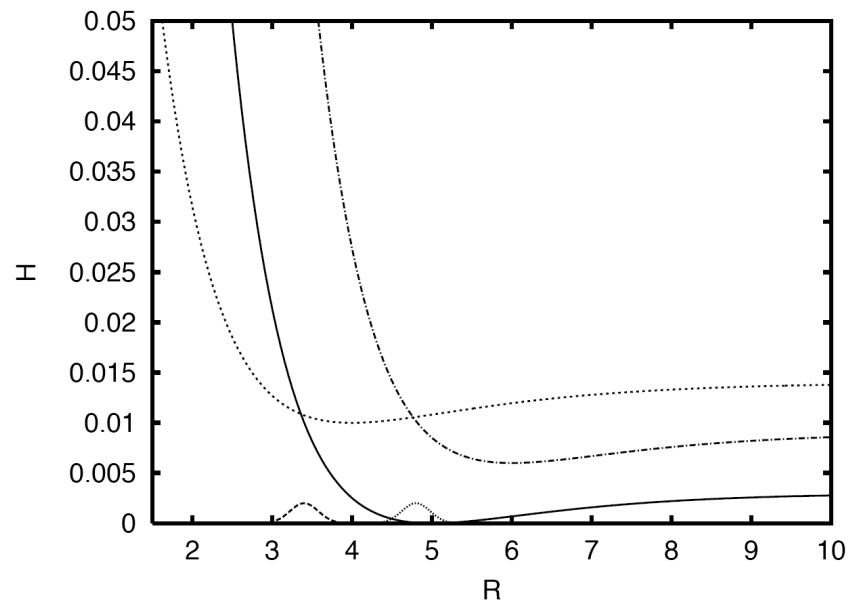
Time dependence of density matrix elements for Stuekelberg scattering $k=30$



Trajectory weight distributions for Stuekelberg scattering $k=30$



Three Coupled Morse Molecular Photodissociation Model



40 hop attempts, $N_{\text{traj}} = 5 \times 10^4, 5 \times 10^5$

Asymmetric spin Boson

$$\hat{\rho}(0) = \hat{\rho}_s(0)\hat{\rho}_b(0)$$

$$H = \frac{1}{2} \sum_{j=1}^M (P^2 + \omega^2 R^2) + \epsilon \hat{\sigma}_z + \hat{\sigma}_z \sum_{j=1}^M g_j R_j - \Omega \hat{\sigma}_x$$

$$J(\omega) = \xi \omega e^{-\omega/\omega_c}$$

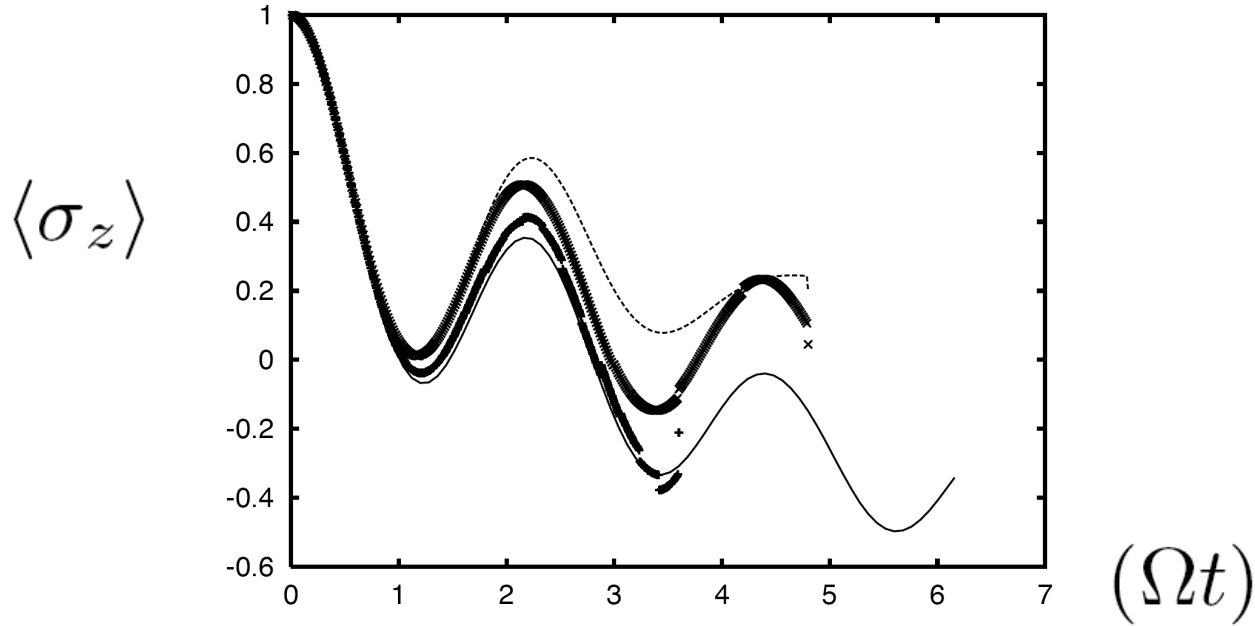


FIG. 9: Population difference $\langle \sigma_z \rangle$ as a function of reduced time (Ωt) for the asymmetric spin-boson with $\xi = 0.13$, $\Omega = 0.4$, $\beta = 12.5$, and $\epsilon = 0.4$, modeled using a discrete bath of 10 oscillators with frequencies sampled from the exponential distribution $\omega_c = 1$ and $\omega_{max} = 3$ (see text). Solid curve gives exact results obtained from MCTDH calculations, dashed curve are linearized dynamics calculations for the full time interval. “x” symbols present results obtained with the iterative linearized scheme using a hop attempt rate of ~ 1.6 , “+” symbols give results using a hop attempt rate of ~ 5.5

Symmetric spin Boson

$$\hat{\rho}(0) = \hat{\rho}_s(0)\hat{\rho}_b(0)$$

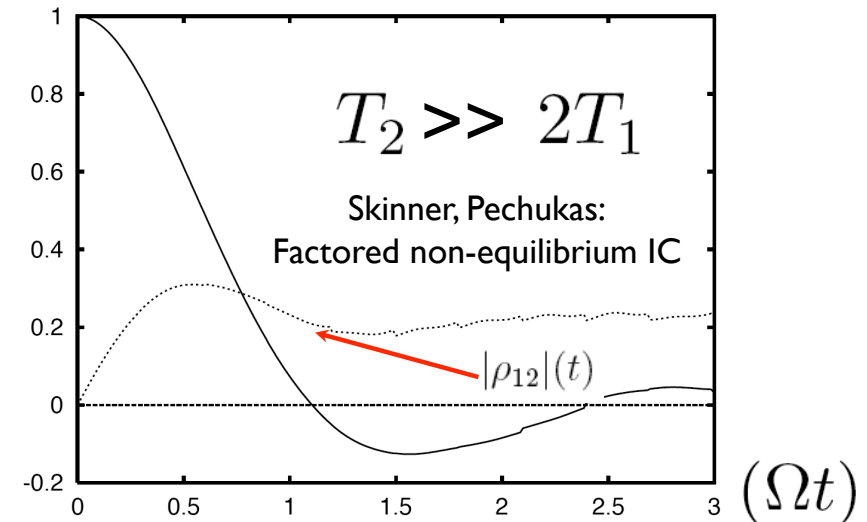
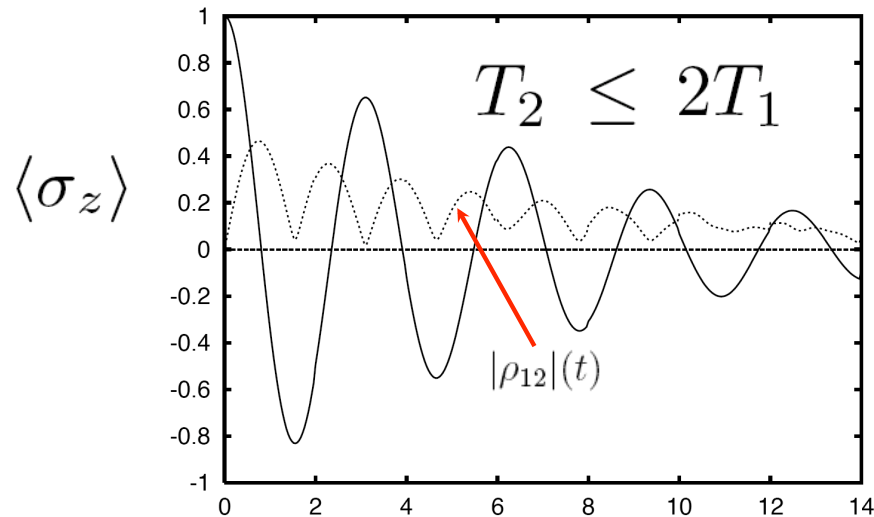
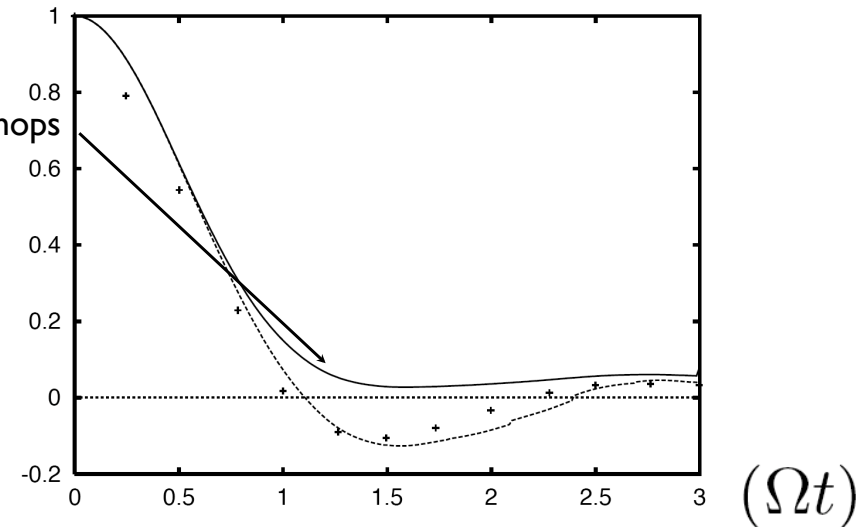
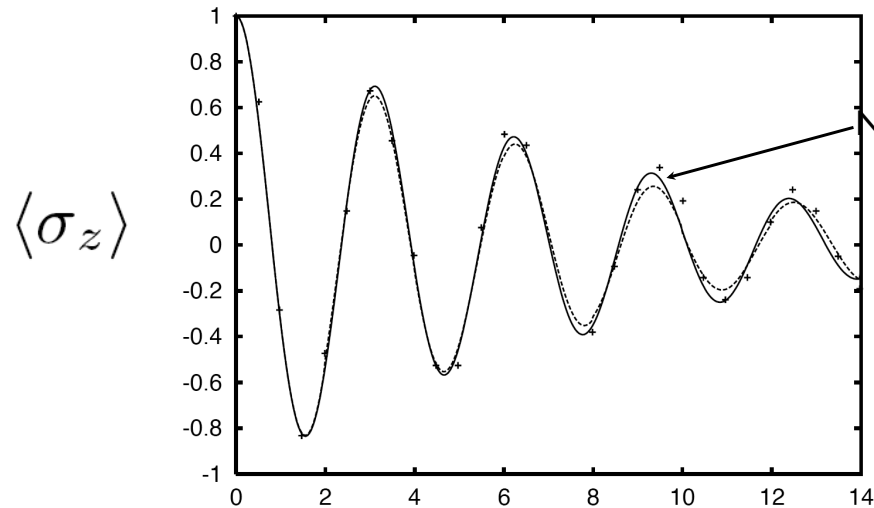
Equilibrium Perturbation Theory

$$1/T_2 = 1/2T_1 + 1/T_2^*$$

$$H = \frac{1}{2} \sum_{j=1}^M (P^2 + \omega^2 R^2) + \hat{\sigma}_z + \hat{\sigma}_z \sum_{j=1}^M g_j R_j - \Omega \hat{\sigma}_x$$

$$\xi = 0.09, \Omega = 0.4, \beta = 12.5$$

$$\xi = 0.5, \Omega = 0.333, \beta = 3.$$



Coherence Dynamics in Photosynthesis: Protein Protection of Excitonic Coherence

Hohjai Lee, Yuan-Chung Cheng, Graham R. Fleming*

Science, 316, 1462 (2007)

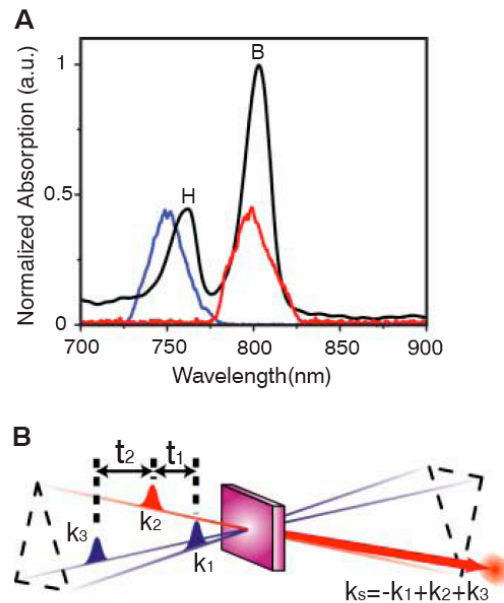


Fig. 1. The 2CECPE experiment. **(A)** The 77 K absorption spectrum (black) of the P-oxidized RC from the photosynthetic purple bacterium *R. sphaeroides* and the spectral profiles of the ~40-fs laser pulses (blue, 750 nm; red, 800 nm) used in the experiment. **(B)** The pulse sequence for the 2CECPE experiment. We detect the integrated intensity in the phase-matched direction $k_s = -k_1 + k_2 + k_3$. a.u., arbitrary units.

states. We applied the method to the coherence between bacteriopheophytin and accessory bacteriochlorophyll in the purple bacteria reaction center (RC). The measurement quantifies dephasing dynamics in the system and provides strong evidence that the collective long-range electrostatic response of the protein environment to the electronic excitations is responsible for the long-lasting quantum coherence. In other words, the protein environment protects electronic coherences and plays a role in the optimization of excitation energy transfer in photosynthetic complexes.

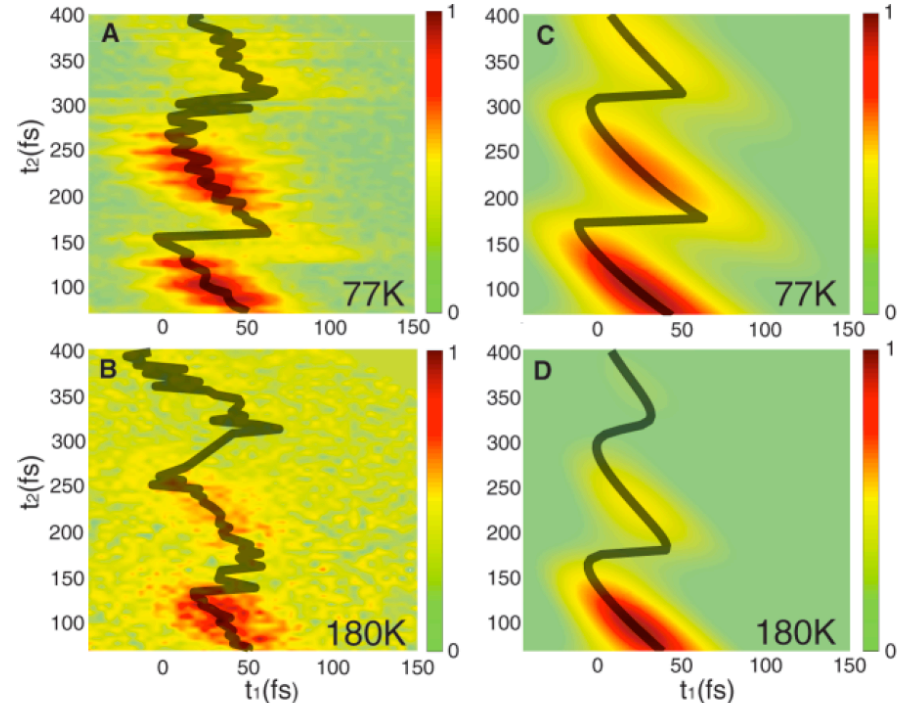
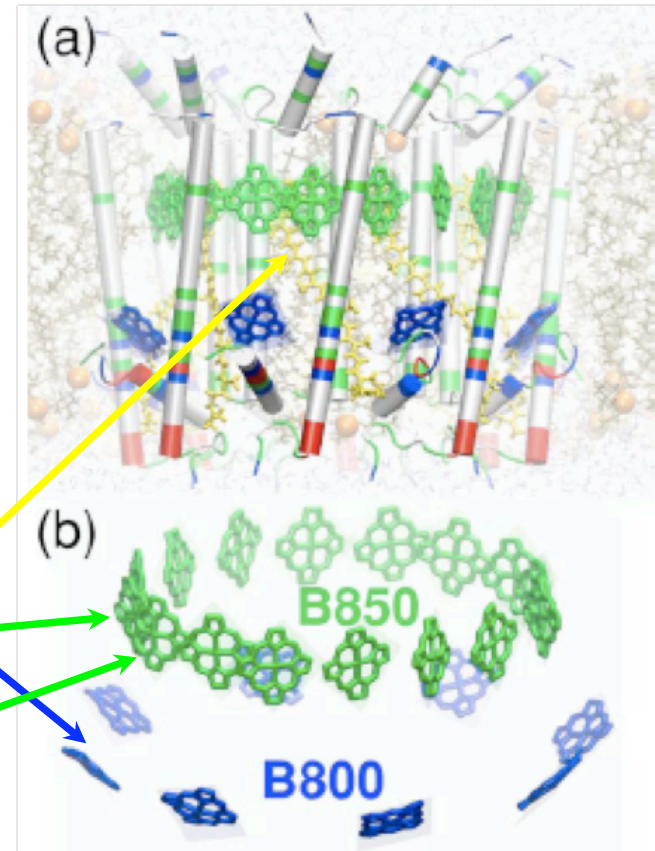


Fig. 2. Two-dimensional maps of experimental **(A and B)** and simulated **(C and D)** integrated echo signals as a function of the two delay times, t_1 and t_2 , from the RC. The black lines follow the maximum of the echo signal at a given t_2 . The data at $t_2 < 75$ fs are not shown because the conventional two-color three-pulse photon echo signal (750-750-800 nm) overwhelms the 2CECPE signal in this region, due to the pulse overlap effect.

“Spin-Boson” model for exciton transport, dissipation, and decoherence in antenna arrays

$$\begin{aligned}
 \hat{H} = & \sum_n \hbar \omega_n (\hat{b}_n^\dagger \hat{b}_n + 1/2) \\
 & + [\epsilon_D + \sum_n \hbar g_{n,D} (\hat{b}_n + \hat{b}_n^\dagger)] |D\rangle \langle D| \\
 & + [\epsilon_\alpha + \sum_n \hbar g_{n,\alpha} (\hat{b}_n + \hat{b}_n^\dagger)] |A_\alpha\rangle \langle A_\alpha| \\
 & + [\epsilon_\beta + \sum_n \hbar g_{n,\beta} (\hat{b}_n + \hat{b}_n^\dagger)] |A_\beta\rangle \langle A_\beta| \\
 & + [\Delta_{\alpha\beta} + \sum_n \hbar g_{n,\alpha\beta}^\Delta (\hat{b}_n + \hat{b}_n^\dagger)] (|A_\alpha\rangle \langle A_\beta| + |A_\beta\rangle \langle A_\alpha|) \\
 & + [J_{D\alpha} + \sum_n \hbar g_{n,\alpha}^J (\hat{b}_n + \hat{b}_n^\dagger)] (|D\rangle \langle A_\alpha| + |A_\alpha\rangle \langle D|) \\
 & + [J_{D\beta} + \sum_n \hbar g_{n,\beta}^J (\hat{b}_n + \hat{b}_n^\dagger)] (|D\rangle \langle A_\beta| + |A_\beta\rangle \langle D|)
 \end{aligned}$$



LHC2

c.f. Jang, Newton, Silbey
J. Phys. Chem. B, 111, 6807 (2007)

$$J_{D\alpha} = \frac{\mu_D \cdot \mu_\alpha - 3(\mu_D \cdot \hat{R}_{D\alpha})(\mu_\alpha \cdot \hat{R}_{D\alpha})}{\epsilon R_{D\alpha}^3}$$

Conclusions:

- (1) Iterative linearized density matrix propagation provides a successively correctible trajectory based mixed quantum-classical dynamics method that can represent environmental coherence effects.
- (2) These methods can probe the mechanism underlying long-lived quantum coherent excited state dynamics e.g. photosynthetic antenna arrays, quantum computing applications.
- (3) Iterating “short” time linearized propagators for long time density matrix dynamics, Monte Carlo density matrix element sampling & taming the exponential growth of trajectories.